3D RF Coil Design Considerations for MRI

Mohammadreza Shiravi[1] and Babak Ganji[1,*]

[1]Department of Electrical Engineering, University of Kashan, Kashan, Iran.

*Corresponding Author's Information: bganji@kashanu.ac.ir

ARTICLE INFO

ABSTRACT

High-frequency coils are widely used in medical applications, such as Magnetic Resonance Imaging (MRI) systems. A typical medical MRI includes a local radio frequency transmit/receive coil. This coil is designed for maximum energy transfer or wave transfer through magnetic resonance. Mutual inductance is a dynamic parameter that determines the energy quantity to be transferred wirelessly by electromagnetic coupling. Thus, it is essential to analyze the self and mutual inductances of this coil. Other parameters, including electromagnetic shielding, frequency, and distance, which influence voltage and power transfer are investigated here. Theoretical formulas and simulation models proposed in the present paper are implemented by using MATLAB and ANSYS MAXWELL and ANSYS SIMPLORER Finite Element (FE) packages for determining the performance and properties of the coil. So, the main goal is evaluating of software steps that simplify the design of RF resonance circuits. Also, experimental results are given for the validation of the proposed method. Consequently, Safety and efficiency are automatically maximized by following the best design considerations.

1. INTRODUCTION

Much research has been carried out in recent years on radio frequency (RF) coil design [1]. Wireless energy transfer has recently been applied to medical devices. However, designing wireless systems is complicated due to the variability of conditions but it is valuable to focus on methods that can sense variations of these systems [2]. It should be noted that the maximum efficiency design is different from the maximum power transfer design because the efficiency concept overlaps with power transfer definition.

By using a power amplifier, efficiency is then maximized to minimize the power loss occurring in circuits [3]. The received power is tracked in [4] by tuning and getting feedback versus the variation of coupling and load impedance with zero voltage switching (ZVS) method, using the switch transistor drain voltage on the transmitter [4]. Another tuning approach is duty cycling by the buck-boost converter.

Switched capacitor banks have also been implemented in [5] to set appropriate capacitance. Resonance frequency variation is also followed for tuning impedance and sensing output voltage feedback by switched capacitance [6]. Separation distance and alignment variations can lead to the change of coupling and power transfer [7].

Therefore, the maximum efficiency point tracking is needed to wirelessly transfer power using magnetic resonant coupling [8]. In [9], a frequency independent configuration has been established for RF coils through DC excitation. Also, 3-D finite element (FE) transient analysis has been carried out using Maxwell in the thick segmented solenoid.

In addition, the RF coil is investigated at the resonance frequency and the external resonant circuit is then designed to achieve the maximum power transfer. Inductive power transfer is a well-known method that can be applied for wireless transfer between the transmitter (Tx) and the receiver (Rx)

through air core, e.g., primary and the secondary transformer windings wrapped around the iron core [10].

The purpose of this paper is to describe and examine some RF coil design problems. One problem is to maximize the power transfer between transmitter and receiver. This can be done by applying resonance circuit through a proper capacitance. Another problem is to reduce the distance between transmitter and receiver.

A third problem is to determine the concept of transferring power and data wirelessly. This can be done by considering shape, amplitude, and frequency of the signal, as well as ambient conditions like noise, temperature and static magnetic field density values. In the MRI systems, the transmitter and receiver coils should not be near to each other. By increasing the distance, the power transfer is also reduced.

The solution is to use electrodes or multi-channel coils to apply resonant circuits to coils for the improvement of the energy transfer.

The next problem is the selection of the coil structure type, i.e., the cylindrical or spiral one. This affects self/mutual inductance of coils and winding design, including the shape of wire cross-section and insulation thickness, coil skew, and the gap between wires. The mutual inductance between two coils determines the value of energy transferred. Development of a practical method for calculating the inductances is the first step of coil design that is also considered in the present paper.

Next, application of coil should be clarified, i.e., whether it is a transmitter, a receivera or both. The RF, gradient and body coils are ordinarily made for both of them. But if a coil is tested in the lab in isolation, two coils have to be considered to prove the idea of the maximum power transfer. It is possible to consider the body cells as coils, but this depends on the modelling of body cells in the Maxwell modeller and thus, it is not feasible.

Therefore, two coils are considered. This is the idea used in this paper, i.e. modelling a sample with an RLC circuit that has not been used elsewhere. Shielding effectiveness is another concept that can help to prove this idea [11].

Some questions related to its material, location, type and size should be answered. The values of electric conductivity, magnetic permeability and mechanic stiffness factor have to be determined. By shielding, it is possible to change inductance, because the electromagnetic (EM) flux does not leak through space.

Another question is whether the core and the shield should be applied for the same goal. It is possible to do this, but the wire is not wrapped around the shield in such cases. The shield geometry depends on the coil

structure. For instance, the planar shield is used for spiral coils (SCs). This introduces a new making which it is possible to make the printed circuit board (PCB) [12-16] for RF appliance, which has not been seen anywhere. It is also possible to make a spherical board to match the sample because of the facilitation property.

In this paper, as the first phase, MRI structure is explained. Next, inductance concept is analyzed and calculated. Then inductances simulated by MATLAB are compared with MAXWELL results, as compliance of relations could be approximately confirmed by these simulations.

In this stage, the inductance calculator technique is specified in Maxwell and it is used in the calculation of the required capacitor at the resonant frequency.

The mentioned idea facilitates one of the main stages of the coil design process. Then resonance and shielding effects on induced voltage can be analyzed and simulated. At the end, some experimental results achieved at the lab are assessed.

Finally, this point should be taken into account that in real condition only one coil is used for both sending and receiving RF signal. The second coil is, in fact, the sample under the cover of the first coil, which it also receives and transmits.

2. MRI SCANNER COMPONENTS

The MRI scanner produces three types of magnetic fields that interact with the proton spins to produce images. The first, the primary field B0 is generated by a superconducting coil surrounded by liquid helium (label A in Fig. 1).

The parameter B0 is the static field directed axially through the scanner tunnel that causes spin precession and the net magnetization of each voxel. Ideally, the main magnet in the scanner will produce a uniform B0 field throughout the entire imaging volume. Since this is a rare case in a commercial scanner, shim coils (label B in Fig. 1) are strategically installed to broaden the region of uniformity.

The shim coils themselves produce magnetic fields that interact with B0 by superposition to correct known field inhomogeneities. The second type of magnetic field applied by the scanner is an RF pulse referred to as the B1 field. This field is produced by the body coil within the scanner (label D in Fig. 1) or by a transmit coil local to the imaging volume (label E in Fig. 1). Finally, the third type of field in the scanner is produced by a specially-designed coil within the scanner called the gradient coil (label C in Fig. 1). When activated, this coil generates three different gradient fields that combine with the primaryB0 field by superposition [13-15].
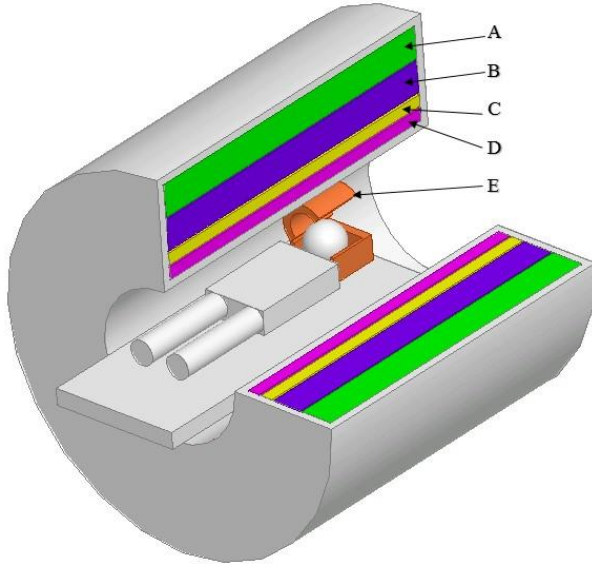
Figure 1: Cut-away view of an MRI scanner, A: Primary field magnet in liquid helium bath, B: Shim coil, C: Gradient coil, D: Body transmit/receive coil, E: Local transmit/receive coil.

3. DETERMINATION OF INDUCTANCES

Let us consider a coil with T turns each carrying a current of I_z. In the case that the effective permeance of flux paths is shown with parameter Λ, the inductance can be derived as follows for a thin coil [16]:

$$L = \frac{T\varphi}{I_z} = \frac{T\,(TI_z\Lambda)}{I_z} = T^2\Lambda \tag{1}$$

Considering length and area of passing flux, the permeance of a tube with height dx at a distance x from the bottom of the conductors is obtained using the equation below [16]:

$$\delta\Lambda = \mu_0 \frac{l\delta x}{W_s} \tag{2}$$

where W_s is the length of flux path, $l\delta x$ is its surface and μ_0 is free space permeability. By integrating (2), permeance related to the whole of field (Λ) is then obtained. To determine the inductance of a single-turn wire loop in H, the following equation is usually used for small wires. The classical solution that includes elliptic integrals is required when the wire is large [17].

$$L = \mu_0 a \left[\ln\left(\frac{8a}{r_0}\right) - 1.75 \right] \tag{3}$$

where a is coil radius, r_0 is wire radius and L is self-inductance in the air. Relation to Magnet coil design, the design of MRI magnet structures is complicated. In the design of conventional magnet structures, the analyst solves a direct problem in which the geometry and magnetization are given and field distribution is then determined. In MRI, the analyst is faced with a more complicated problem in which field strength and uniformity are determined across the imaging region and the geometry and magnetization of the structure need to be identified. There is no unique solution for such problems in that a specified field distribution within a closed region can be obtained using an infinite number of different structures [18].

4. THEORETICAL ANALYSIS

By [19] and [20], which are well-known works on providing inductance tables in the past and recent years, we can test the results of analytical and experimental works in this field. In recent years, numerous papers have been published on the problem of calculating mutual inductance by analytical methods such as [21]-[26]. Equation (4) has been developed to calculate the mutual inductance between coaxial single-turn coils without any limitations in dimension (it means considering rectangular cross-section), taking into account the effect of overlap, in [21]. In [22], the procedure for calculation of mutual inductance is presented in the filament method, and then the magnetic field is extracted for coaxial circular coils. The accurate approach is proposed for calculation of mutual inductance between inclined coils and non-coaxial coils (with a rectangular cross-section or negligible section) respectively in [23] and [24]. At [25], the filament method was used to calculate the mutual inductance and a rectangular or negligible cross section was assumed. This shows the calculation of the mutual inductance for a specific application. Both coaxial and non-coaxial coils are analyzed for the self-inductance and mutual inductance calculation by Bessel functions in [26]. In the first theory, the mutual inductance in (4) between two planar coils is extracted from Maxwell's equations is reported in [10-11, 21, 27].

$$M = \frac{\mu_0\pi}{h_1 h_2 \ln\left(\frac{r_2}{r_1}\right)\ln\left(\frac{a_2}{a_1}\right)}$$
$$\cdot \int_0^\infty S(kr_2, kr_1)\,S(ka_2, ka_1)\,Q(kh_1, kh_2)\,e^{-k|d_2 - d_1|}\,dk \tag{4}$$

as it is shown in Fig. 2, h_1 and h_2 are the thicknesses of winding tracks, a_1 and r_1 are internal radii of circular windings, a_2 and r_2 are external radii of circular windings. d_1 and d_2 are the heights of two planar coils or winding centers above the substrate. The parameter k is a variable for integration and it is essential for the definition of Bessel functions. The parameter M is mutual inductance between planar

windings in the air in the absence of the substrate. The parameters $Q(kx, ky)$ and $S(kx, ky)$ in (4) are defined as follows:

$$Q(kx,ky) = \frac{2}{k}\left(h + \frac{e^{-kh}-1}{k}\right), z=0, x=y=h \tag{5}$$

$$S(kx,ky) = \frac{J_0(kx) - J_0(ky)}{k} \tag{6}$$

where $J_0(x)$ is a first kind Bessel function. The mutual inductance is calculated from Table 1 which is extracted by MATLAB code by adding 'syms x' command in the first line of code in [10]. The discrepancy between mutual inductances at this work and [10] is zero. In this Table, r_1 and a_1 are inner radii of coils, r_2 and a_2 are outer radii of coils and M is the mutual inductance between two coils.

Calculation of the Mutual inductance of two cylindrical coils is more complicated which is illustrated in [28]. In Fig. 3, dimensions of the two coils are shown. At the following, the objective is to show the simplicity of Maxwell simulation method versus analytical calculation which is proposed in [28].
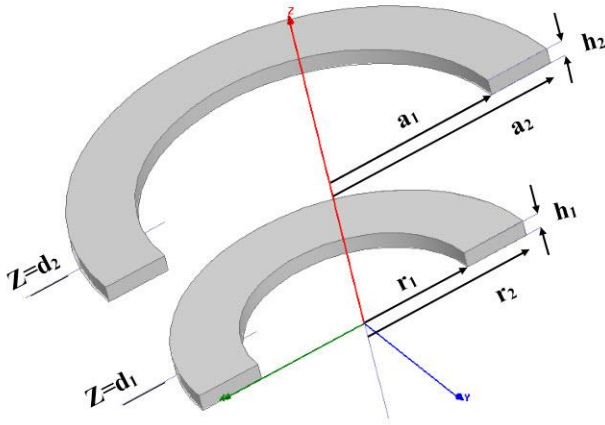

Figure 2: The parameters related to the two planar coils.

TABLE 1
THE DEFINED PARAMETERS

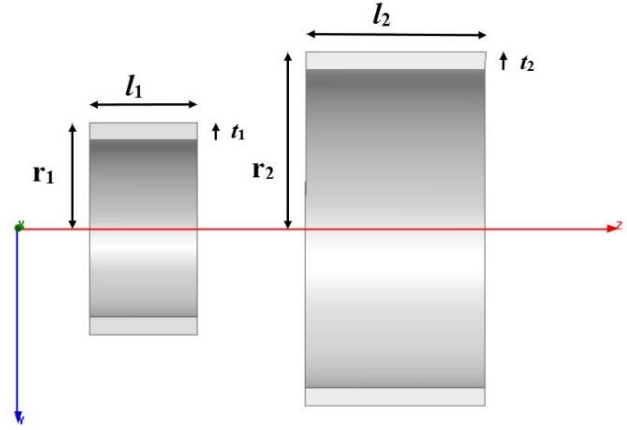| a1 [mm]	a2 [mm]	r1 [mm]	r2 [mm]	M [H]
2.6	3	3.6	4	5.4252e-09
2.6	3	5.6	6	2.9427e-09
2.6	3	7.6	8	2.0867e-09
2.6	3	9.6	10	1.6487e-09
2.6	3	11.6	12	1.3640e-09

Figure 3: The parameters considered for the two cylindrical coils.

It should be considered that if two coils with equal dimensions are selected, then M will be greater. Similarly, in the case that two coils with different sizes are selected, M will be smaller. If it is assumed that flat SC is combined with N turns, its inductance is then is calculated by following equation [10]:

$$L = \frac{r^2 N^2}{8r + 11D} \tag{7}$$

where L is inductance in μH, r (inch) is the mean radius of the coil, N is a number of turns, and D is the depth of coil derived from outer radius minus inner radius. The formula of inductance L for a short air-core cylindrical coil (CC) is as follows [10]:

$$L = \frac{r^2 N^2}{9r + 10l} \tag{8}$$

where N is the number of turns, r (inch) is the outer radius of the coil, l (inch) is the length of the coil. In the second step, two identical CC is used as a Tx and Rx pairs. Ignoring high-frequency effects and skin effect, it is proved that the maximum power is transferred in resonance mode, and the value of capacitance is calculated using the equation below [10]:

$$C = \frac{1}{4\pi^2 f^2 L} \tag{9}$$

where f is the frequency of power supply, C is capacitance in F and resistance of components is neglected. Adding C parallel to Tx and Rx, it is seen that the induced voltage in R, becomes greater. It should be noted that output voltage is derived from voltage division as follows [10]:

$$V_O = \frac{\dfrac{1}{j\omega C}}{R_C + j\omega L + \dfrac{1}{j\omega C}} V_S \tag{10}$$

where R_C is the resistance of capacitor and V_S is a voltage induced in the receiver coil.

A. Simulation results

The first step in coil design is carried out by obtaining coil inductance. For this, a 3D model is drawn and the magnetostatic solution is set up. For 3D model, a number of steps are done. It is important to assign "parameters" as a matrix. Next, the model is analyzed, data can be seen on Maxwell 3D inductance matrix. This matrix is used in the capacitance design for resonance circuit.

B. Extracting Inductance

On the basis of the previous section, the mutual inductance value of two flat coils in Fig. 2, is determined by a 3D model, which is shown in Figure 4. As it is seen in Table 2, the difference of mutual values (calculated by MATLAB code: 1.3640e-09 H and Maxwell value: 1.3344E-009 H) is the only 2.17% which is acceptable.
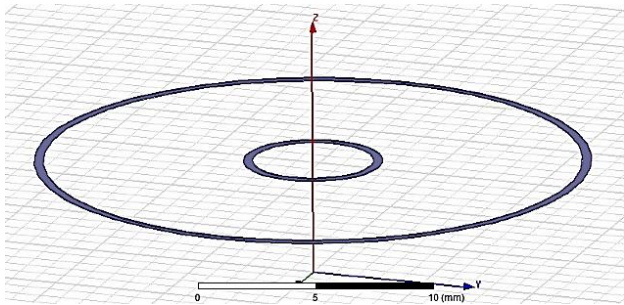

Figure 4: Two flat coils: r2 = 12 mm, r1 = 11.6 mm, a2 = 3 mm, a1 = 2.6 mm and h1 = h2 = 0.035 mm.

TABLE 2
SELF AND MUTUAL INDUCTANCES

	Coil 1	Coil 2
Coil 1	1.762e-8	1.3344e-9
Coil 2	1.3344e-9	8.8564e-8

C. Resonance Effect and Induced Voltage

The second step is done in the transient mode of solution setup. In this state, the induced voltage of the receiver coil is analyzed, and the impact factors are identified. For a transient solution, coil terminal and winding are also assigned. Winding source type can be assigned as external or internal (current or voltage) and as AC or DC. In the external mode (designing circuit in circuit editor), it is possible to use a resonance circuit. As an example, the inductance of CC is calculated (formula: L= 9.28 μH, Maxwell3D: 0.11 μH, as shown in Table 3, resulting from magnetostatic analysis). It is noted that Fig. 5 is related to Table 3. The reason for the difference between these values is that it doesn't consider the realistic conditions. The results pertaining to the resonance circuit, by

transient analysis, also helped us to select the best value. The important question in this part is what should be done with the configuration (for R, L, C and source in the transmitting side and R, L and C in the receiving side) that should be assigned. What is the role of resistance? After doing some tests, the configuration which is shown in Fig. 6 is selected as an external excitation circuit. By some tests based on (8) and (9), C = 0.618 pF is added to the receiver and transmitter to produce a maximum voltage across the receiver via the resonance frequency which is 64 MHz by a sinusoidal voltage source (1mv@64MHz). The voltages related to different values of C including 0.618, 25, and 56 pF have been shown in Fig. 7, Fig. 8, and Fig. 9, respectively. Based on Maxwell value of L = 0.11 μH, the calculation of C = 56 pF has been completed. In this case, the receiver voltage is greater than that of the transmitter. When the external circuit is used without capacitance, the receiver voltage is 0.0479 mv, which is shown in Fig. 10 by 10-fold magnification.
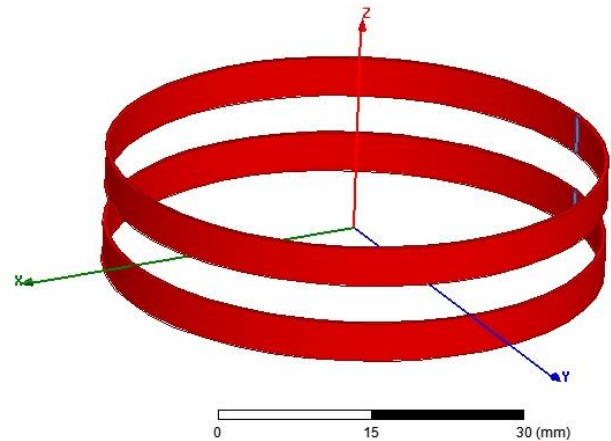

Figure 5: Maxwell3D design for CC and its inductance: r=r_1=r_2 = 25 mm, l=l_1=l_2 = 4 mm, thickness = 0.4 mm.

TABLE 3
SELF AND MUTUAL INDUCTANCES

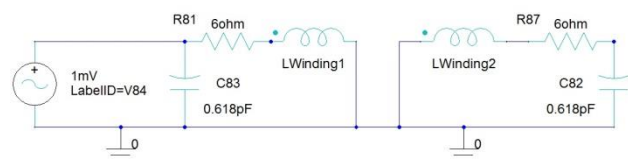|	Coil 1	Coil 2
Coil 1	1.0937e-7 H	3.9458e-8 H
Coil 2	3.9458e-8 H	1.1059e-7 H

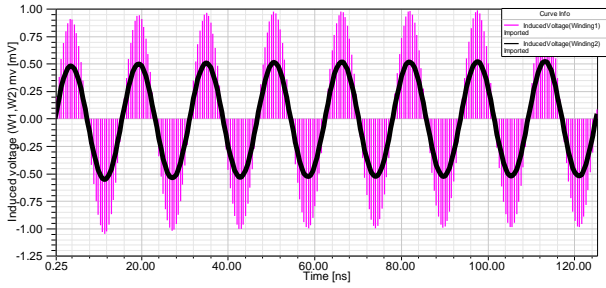Figure 6: External circuit for excitation of the two cylindrical coils.

Figure 7: Induced voltages of Tx and Rx windings for c = 0.618 pF.
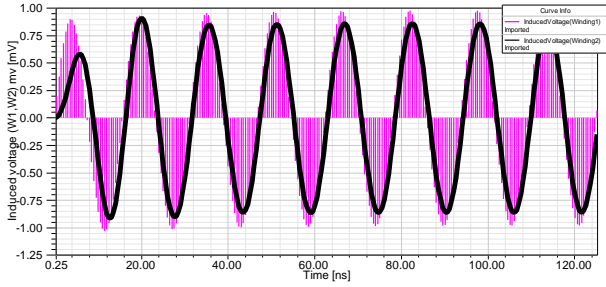

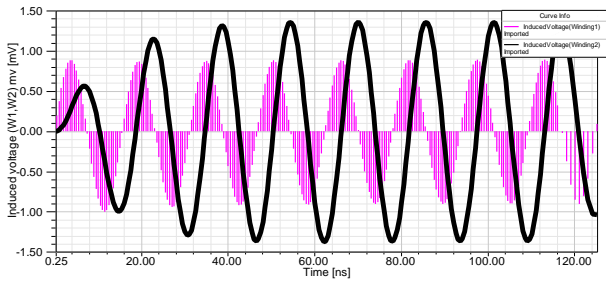Figure 8: Induced voltages of Tx and Rx windings for c = 25 pF.

Figure 9: Induced voltages of Tx and Rx windings for c = 56 pF based on L = 0.11 μH.

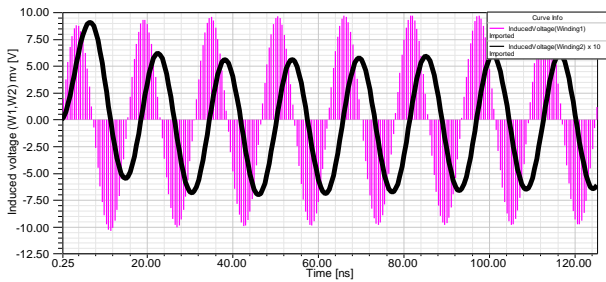Figure 10: Induced voltages of Tx. and Rx. windings without capacitance, R = 6 Ω, V_s=10 v.

D. Wireless Power Transfer Efficiency

Here, ANSYS Simplorer 11.0 is used instead of ANSYS Maxwell Circuit Editor. Again, excitation circuit which is shown in Fig. 11, is drown in Simplorer. Middle block is Maxwell component which is added as a dynamic inductance. Then, Ac source, capacitance and resistance value should be set. Now Ac analysis is setup. In Fig. 12 and Fig. 13, in the result, wireless power transfer efficiency with linear and logarithm axis scaling is shown.
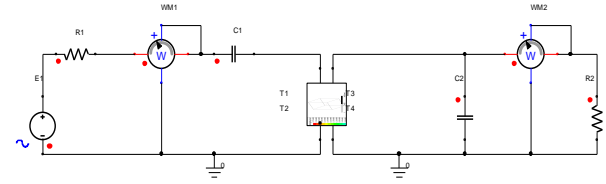

Figure 11: simulation of power transfer efficiency by Ansys Simplorer. Middle block is Maxwell component which consists Tx and Rx coil in magnetostatic solution mode which is added as a dynamic inductance. As it is seen for this condition, resonance frequency occurs at 20.7405 MHz. at resonance frequency maximum transfer power ratio is 0.9160.
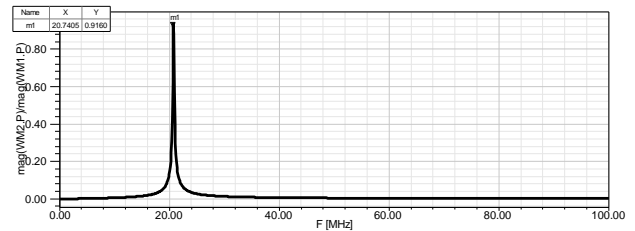

Figure 12: Wireless power transfer efficiency with linear axis scaling.
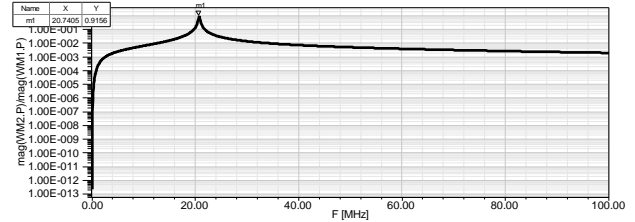

Figure 13: Wireless power transfer efficiency with logarithm axis scaling.

E. Shielding Effectiveness

The low voltage of 1 mV is blocked by permanent magnet NdFe35 shield plate at a distance of 1 mm. The voltage value is then set to 10 V. Another point is that if CC could be analyzed in magnetostatic solution and its matrix parameters must be eliminated. It is now possible to do sampling from the axial magnetic field by drawing a line along the coil axis. The position of two NdFe35 plates is at a distance of 1 mm above and below the CC pair.

Its magnetic field density is shown in Fig. 14 in solid line where two squares show this position's the effect of two PM plates. The dotted line is magnetic field density of two coils with non-PM plates by zoom in 2500 times greater. By increasing the distance between plates to 100 mm and 1000 mm, axial magnetic fields are found to be 0.0031 T and 0.0006 T, respectively. Based on works have been done in [12], the shielding effectiveness (SE) formula is (11), which is the amplified decibel-receiving voltage ratio of unshielded to the shielded case.

$$SE = 20log\frac{E_1}{E_2} \tag{11}$$

$$\omega_0 = \sqrt{\frac{1}{LC} - \left(\frac{R_L}{L}\right)^2} \tag{12}$$

where E_1 and E_2 are received voltage values without and with the material present, respectively. This equation is proved by some experimental results in [10]. The effect of thickness, material, and a layer of shield and voltage source frequency on the inductance value is also analyzed in [29, 30]. This means that the work can be done in magnetostatic solution.
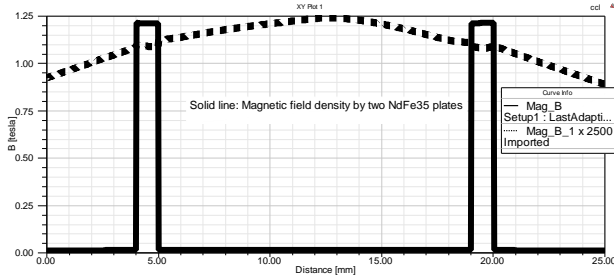
$$Z(\omega_0) = \frac{RL}{R_L RC + L} \tag{13}$$

$$V_0(\omega_0) = |I_s(\omega_0)|\frac{RL}{R_L RC + L} \tag{14}$$

In this case, the voltage amplitude is not the maximum at ω_0 but it is the maximum at ω_m which is:

$$\omega = \omega_m = (x - y)^{0.5} \tag{15}$$

Figure 14: Axial magnetic field density. Distance is the length that is placed on the axis of two coils.

$$x = (a+b)^{0.5}, a = \frac{1}{(LC)^2}\left(1 + 2\frac{R_L}{R}\right)$$
$$, \quad b = \left(\frac{R_L}{L}\right)^2\frac{2}{LC}, y = \left(\frac{R_L}{L}\right)^2 \tag{16}$$

5. EXPERIMENTAL RESULTS

A. Tightening and adjusting the resonance frequency

Equation (7) to (11) are proved by using the experimental results of two coils in [10] and [31] and four coils in [32-34]. In our paper, these experiments are done by an oscilloscope (Gw INSTEK GOS-635G) and the function generator (Gw INSTEK SFG-2104). The theoretical analyses are then validated by the measurements carried out. Changing the volume frequency, the resonance frequency for the given coils and capacitance pairs is determined. At the first, the CC pairs described in (8), Fig.5 is prepared. Their capacitance is changed to C = 220 pF. By volume tuning, the resonance frequency is found to be f = 2.833 MHz at the laboratory. At this frequency, the maximum voltage is transferred. Based on the laboratory results, the received voltage is considerable. By increasing the distances between the coils based on Table 5, the receiver-induced voltage is decreased. There is a little difference between the calculated and measured values for the resonance frequencies. In order to ensure realistic conditions, the resistance of the inductor should be considered for calculating resonance frequency. In Fig. 15, resonance circuit model is shown. Then, the resonance frequency is extracted by Laplace transform and calculating the inductance. Now, the inductance imaginary part is equalled to zero and (12) is found in [35]. As it is seen, the resonant frequency is dependent on the coil resistance. By replacing (12) in impedance, (13) and (14) are obtained:

This frequency is achieved by differentiating $V_0(\omega_0)$ versus ω_0. The capacitance is now set to C = 470 pF and its resonance frequency is calculated for the parameters: f = 2.1 MHz, d = 50 mm, v_1 = 1.8 V, and v_2 = 1.1 V. In this case, PM shielding is done. A circular PM disc with a diameter of 55 mm and thickness of 10 mm is placed between the two coils. And V_2 is reduced to 0.19 V for which SE is 15.25 dB. For d = 30 mm, v_2 is decreased from 2.8 V to 0.27 V, yielding SE of 20.31 dB.

By increasing frequency to f = 2.28 MHz, v_2 is also increased. The resonance frequency is increased using the PM, but the receiver voltage is decreased. The shifting of the resonance frequency is useful. When the sample is presented, the resonance frequency is shifted. In the case that shielding is considered, the resonance frequency remains unchanged.

This is followed using the effective ferrite plate shield by which the resonance frequency is increased to 2.16 MHz. Through the ferrite plate shielding and d = 30 mm, v_2 is decreased from 2 V to 0.65 V and SE is 9.76 dB. Attenuation of the receiver-induced voltage is clearly validated in both shielding states.

Electromagnetic shielding is a problem inside the MRI but it is a solution outside it. Naturally, we get shielding with distance because electric and magnetic fields and power density are reduced by increasing the distance. Shielding effectiveness is more dependent on geometry rather than on material. If one has an infinitely large metal plate or metal enclosure, one could shield everything. There are two basic experimental methods to measure SE which are waveguide and free space, as reported in [36]. It should be noted that the second method is used in the present paper.

TABLE 4
IMPACT OF DISTANCE ON INDUCED VOLTAGE

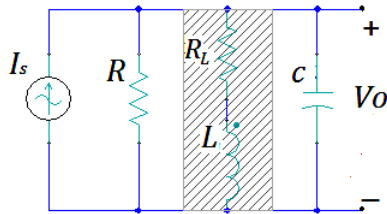| Distance [mm]	V_1	V_2
10	2.4	15.5
20	2.4	8.5
30	2.4	4.2
40	2.4	2.5

Figure 15: Resonance circuit model using realistic inductor.

B. Evaluation of the proposed method in an example RF Transceiver coil

Finally, the PCB is designed for the desired static coil. That is, the values of the capacitance and inductance are dependent on the resonance frequency, and the frequency is dependent on the static coil magnetic field density. In Fig. 16, the PCB which is designed using Proteus software is shown. Here, the tracks are thicker to reduce the effects of noise. It is also possible to abandon the parallel diodes and the Tx connector and use an SMA (RF-BNC) instead of the Rx connector. Parallel capacitor (C_m) and series capacitor (C_t) are used respectively for further matching and tuning and the equation of calculating their values, is mentioned in [37]. The RF coil here is of solenoid type, so that the sample can easily be placed inside it. Here the amount of inductance is calculated using software and measured by RLC-meter (DM4070), and they do not differ significantly. For example, by fixing the static field value equal to $B_0 = 0.12$ (T) and the value of the solenoid coil inductance is equal to L = 6.2 (µH) which is measured by DM4070 (diameter and length of solenoid is respectively 7.5 (mm) and 20 (mm) and with 40 turns, then by simple formula $L = N^2/\Re = 5.05$(µH), and by Maxwell: 5.9 (µH) is achieved (helical coil should be designed not solid cylindrical), which is acceptable), the angular frequency is based on the relation $\omega = \gamma B_0 = 32.1$ (MHz), and the Larmor frequency is f = 5.109 (MHz). Where γ is the gyromagnetic ratio for the proton and is equal to 2.675×10^4 for glycerin. The resistance is assumed to be R = 1.2 (Ω). Interestingly, the coil resistance (measured by DM4070) is $R_L = 0.2$ (Ω) and the external resistance is 1.0 (Ω). And by the equations given in reference [37], C_t and C_m values respectively are achieved as 163 (pF) and 3973 (pF). When the resistance R is assumed to be larger than the above

value, the result will have a less capacity of C_m. And by changing the amount of coil inductance, both C_t and C_m are changed. This means that for a fixed frequency, more than one circuit with different components can be considered.
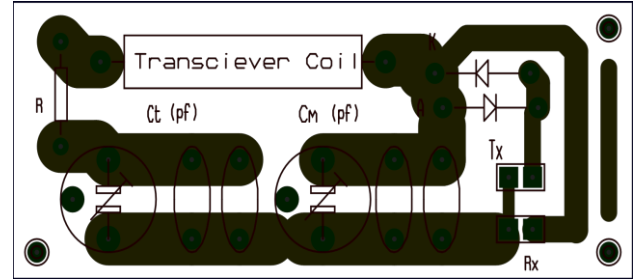

Figure 16: PCB layout which is designed for low-cost MRI.

Figure 17: The final RF resonant circuit.

6. SUMMARY AND CONCLUSION

Due to the priority of Maxwell simulations, in the first step, the magnetostatic solution is found and the inductance is extracted. As seen from Maxwell and MATLAB simulation results, they are nearly close each other. In the second step, the transient solution is analyzed and the receiver-induced voltage is maximized by adding the resonance capacitance across the windings. The capacitance value obtained by the formula is nearly the same as the simulation value. So, it is possible to design all resonance circuits accurately by ANSYS in two steps without using any complicated analytical or numerical methods. Another method for maximizing the induced voltage is reducing the distance. In addition, the effect of distance and shielding is tracked. In this paper, it is generally accepted that electromagnetic shielding plays an important role in RF coil design for MRI. It is also possible to use ANSYS HFSS, in order to obtain the best design e.g. drawing and modelling setup for special RF coils.

7. ACKNOWLEDGEMENTS

REFERENCES

[1] E. Bratschun, D. Tait, and N. Moin, "Next-generation MRI scanner," Colorado State University, Final Project Report, spring 2016.

[2] K. N. Bocan and E. Sejdic, "Adaptive transcutaneous power transfer to implantable devices: A state of the art review," *Sensors*, vol. 16, no. 3, pp. 393, 2016.

[3] S. Y. R. Hui, W. Zhong, and C. K. Lee, "A critical review of recent progress in mid-range wireless power transfer," *IEEE Trans. Power Electronics*, vol. 29, no. 9, pp. 4500–4511, 2014.

[4] D. Ahn and S. Hong, "Wireless power transmission with self-regulated output voltage for biomedical implant," *IEEE Trans. Ind. Electronics*, vol. 61, no. 5, pp. 2225–2235, 2014.

[5] D. Ahn and S. Hong, "Wireless power transfer resonance coupling amplification by load-modulation switching controller," *IEEE Trans. Ind. Electronics*, vol. 62, no. 2, pp. 898–909, 2015.

[6] F. Rodes, M. Zhang, R. Denieport, and X. Wang, "Optimization of the power transfer through human body with an auto-tuning system using a synchronous switched capacitor," *IEEE Transactions on Circuits and Systems II: Express Briefs*, vol. 62, no. 2, pp. 129–133, 2015.

[7] A. A. Danilov and E. A. Mindubaev, "Influence of angular coil displacements on effectiveness of wireless transcutaneous inductive energy," *Transmission Biomed. Eng.*, vol. 49, pp. 171–173, 2015.

[8] H. Li, J. Li, K. Wang, W. Chen, and X. Yang, "A maximum efficiency point tracking control scheme for wireless power transfer systems using magnetic resonant coupling," *IEEE Trans. Power Electronics*, vol. 30, pp. 3998–4008, 2014.

[9] M. S. Khoozani, H. M. Kelk, and A. S. Khoozani, "Comprehension of coils overlapping effect," *Open Access Library Journal*, vol. 2, no. 1, e945, pp. 1-13, January 2015.

[10] R. Dunne, "Electromagnetic shielding techniques for inductive powering applications," Thesis, Galway University, Ireland, 2009.

[11] Y. P. Su, X. Liu, and S. Y. Hui, "Extended theory on the inductance calculation of planar spiral windings including the effect of double-layer electromagnetic shield," *IEEE Trans. Power Electronics*, vol. 23, no. 4, pp. 2052-2061, July 2008.

[12] S. C. Tang, S. Y. Hui, H. Shu, and H. Chung, "Evaluation of the shielding effects on printed-circuit-board transformers using ferrite plates and copper sheets," *IEEE Trans. Power Electronics*, vol. 17, no. 6, pp. 1080-1088, July 2002.

[13] R. P. Merril, A twenty-eight channel coil array for improved optic nerve imaging, The University of Utah, May 2010.

[14] R. Brown and et al., *Magnetic resonance imaging: Physical principles and sequence design*, 2nd ed. Hoboken: John Wiley & Sons, 2014.

[15] P. Rinck, Magnetic resonance, a critical peer-reviewed introduction, Internet: http://www.magnetic-resonance.org, 2016.

[16] A. K. Sawhney: A course in electrical machine design, Dhanpat Rai, and Sons, 1970.

[17] W. H. Yeadon and A.W. Yeadon, *Handbook of small electric motors*, McGraw-Hill, 2001.

[18] M. T. Thompson, Inductance calculation techniques, Power Control and Intelligent Motion, December 1999.

[19] H. B. Dwight, "Some new formulas for reactance coils," *Trans. Amer. Inst. Electr. Eng.*, vol. 8, no. 2, pp. 1675–1696, 1919.

[20] F. W. Grover, Inductance Calculations: Working Formulas and Tables, New York, NY, USA: Dover, 2004.

[21] W. G. Hurley, M. C. Duffy, J. Zhang, I. Lope, B. Kunz, and W. H. Wolfle, "A unified approach to the calculation of self- and mutual-inductance for coaxial coils in air," *IEEE Trans. Power Electronics*, vol. 30, no. 11, pp. 6155-6162, November 2015.

[22] C. Akyel, S. I. Babic, and M. Mahmoudi, "Mutual inductance calculation for non-coaxial circular air coils with parallel axes," *Progress In Electromagnetics Research, PIER.*, vol. 91, , pp. 287-301, April 2009.

[23] S. I. Babic and C. Akyel, "Calculating mutual inductance between circular coils with inclined axes in air," *IEEE Trans. Magn.*, vol. 44, no. 7, pp. 1743 – 1750, 2008.

[24] C. Akyel, S. I. Babic, and M. M. Mahmoudi, "Mutual inductance calculation for non-coaxial circular air coils with parallel axes," *Progress in Electromagnetics Research*, PIER 91, pp. 287–301, 2009.

[25] M. R. Alizadeh Pahlavani and A. Shiri, "Impact of dimensional parameters on mutual inductance of individual toroidal coils analytical and finite element methods applicable to Tokamak reactors," *Progress in Electromagnetics Research B*, vol. 24, pp. 63-78, 2010.

[26] J. T. Conway, "Inductance calculations for non-coaxial coils using Bessel functions," *IEEE Trans. Magn.*, vol. 43, no. 3, pp. 1023-1034, 2007.

[27] W. G. Hurley and M. C. Duffy, "Calculation of self and mutual impedances in planar sandwich inductors," *IEEE Trans. Magn.*, vol. 33, no. 3, pp. 2282-2290, May 1997.

[28] T. H. Fawzi and P. E. Burke, "The accurate computation of self and mutual inductances of circular coils," *IEEE Trans. Power App. and Systems,* vol. PAS-97, no.2, pp. 464 – 468, 1978.

[29] X. Liu and S. Y. R. Hui, "Optimal design of a hybrid winding structure for planar contactless battery charging platform," in *Proc. 2006 IEEE Industry Applications Conference Forty-First IAS Annual Meeting*, pp. 2568-2575, 2006.

[30] X. Liu, and S. Y. R. Hui, "An analysis of a double-layer electromagnetic shield for a universal contactless battery charging platform," in *Proc. 2005 IEEE 36th Power Electronics Specialists Conference*, pp. 1767-1772, 2005.

[31] H. W. Secor, Tesla apparatus and experiments-how to build both large and small Tesla and Oudin coils and how to carry on spectacular experiments with them, Practical Electrics, 1921.

[32] T. P. Duong and J. W. Lee, "Experimental results of high-efficiency resonant coupling wireless power transfer using a variable coupling method," *IEEE Microw. Wireless Compon. Lett.*, vol. 21, no. 8, pp. 442–444, Aug. 2011.

[33] A. Kurs, A. Karalis, R. Moffatt, J.D. Joannopoulos, P. Fisher, and M. Soljacic, "Wireless power transfer via strongly coupled magnetic resonances," *Science*, vol. 317, pp. 83–86, Jul 2007.

[34] T. Miyamoto, Y. Uramoto, K. Mori, H. Wada, and T. Hashiguchi: Wireless charging system, U.S. Patent Appl. 20 120 038 317, Feb. 2012.

[35] J. Edlinger and J. Steinschaden, "Simulation and Characterization of a Miniaturized Planar Coil," Thesis, Vorarlberg University, Aug. 2009.

[36] C. L. Holloway, "Electromagnetic shielding: principles of shielding of planar materials and shielding of enclosures," National Institute of Standards of Technology (NIST), U.S. Department of Commerce, July 2010.

[37] C. L. Zimmerman, "Low-field classroom nuclear magnetic resonance system," Massachusetts Institute of Technology, Feb. 2010.

BIOGRAPHIES:

Mohammadreza Shiravi was born in Esfahan, Iran, on December 1, 1984. He received the B.Sc. degree in electrical engineering from Shahrekord University, Iran, in 2009. He received the M.Sc. degree from Tafresh University, Iran, in 2014 and is currently a Ph.D. student at Kashan University. His special fields of interest included MRI coil design. He has published two papers in ICEEM and PSC

conferences and one paper in OALIB journal, all in MRI coil design field.

Babak Ganji was born in Esfahan, Iran, in 1977. He received the B.Sc. degree in electrical engineering from Esfahan University of Technology, Iran, in 2000. He received the M.Sc. and the Ph.D. degrees from the University of Tehran, Iran, in 2002 and 2008, respectively. In 2006, he was a Visiting Researcher with the Institute for Power Electronics and Electrical Drives, RW TH Aachen University, Aachen, Germany, for a period of six months. This research visit was supported by the DAAD (German Academic Exchange Service). He has been working as a Faculty Member with the Department of Electrical Engineering, University of Kashan, Iran, since February 2009. His research interest is modelling and designing of advanced electric machines.